



## Effective dose comparison between stitched and single FOV in CBCT protocols for complete dental arcade<sup>☆</sup>



Maria Rosangela Soares<sup>a,\*</sup>, Wilson Otto Batista<sup>b</sup>, Patricia de Lara Antonio<sup>c</sup>,  
Linda V.E. Caldas<sup>c</sup>, Ana F. Maia<sup>a</sup>

<sup>a</sup> Federal University of Sergipe, UFS, NPGFI, Rod. Marechal Rondon s/n, Jardim Rosa Elze, CEP: 49.100-000, São Cristóvão, SE, Brazil

<sup>b</sup> Federal Institute of Bahia, IFBA, Rua Emídio dos Santos, s/n. Barbalho, CEP: 40301015 Salvador, BA, Brazil

<sup>c</sup> Nuclear and Energy Research Institute, IPEN, Av. Lineu Prestes 2242, Cidade Universitária, CEP: 05508-000, São Paulo, SP, Brazil

### HIGHLIGHTS

- The study relies on the comparison of two protocols with similar goals of CBCT: stitched protocols and single protocols.
- The stitched FOV protocol is more specific and it is good option when want imaging only of some dental units.
- In relation the effective dose, single FOV protocols presents advantage over the stitched FOV protocols.
- Know the exposure parameters and effective dose values associated with each image protocol is necessity for request the best CBCT tomographic image.

### ARTICLE INFO

#### Article history:

Received 12 May 2014

Received in revised form

21 December 2014

Accepted 20 January 2015

Available online 22 January 2015

#### Keywords:

CBCT

Effective dose

Stitched-FOV

Single-FOV

Thermoluminescent dosimetry

### ABSTRACT

**Objective:** The objective of this study was to assess and compare protocols with a single field of view and multiple stitched field of view with a similar clinical purpose by means of effective dose value.

**Materials and methods:** Measurements of absorbed dose were performed with thermoluminescent dosimeters inserted in the position of organs/tissues of a female anthropomorphic phantom and from these values the effective dose was calculated, utilizing weighting factor tissue-ICRP 103 (2007).

**Results:** The results obtained in this study for effective dose are within the range of 43.1  $\mu$ Sv and 111.5  $\mu$ Sv for equipment using protocols with single FOV and in the range of 44.5  $\mu$ Sv and 236.2  $\mu$ Sv for equipments that using protocols with stitched field of view.

**Conclusions:** In terms of the value of effective dose, stitched FOV protocols do not have any advantage over the single field of view protocols. This results suggest the necessity for knowledge of the exposure parameters and effective dose values associated with each image protocol.

© 2015 Elsevier Ltd. All rights reserved.

## 1. Introduction

Cone beam computed tomography (CBCT) was introduced into dentistry in the late 1990s (Mozzo et al., 1998). Since its inclusion in dental radiology, this imaging technique has incorporated new technological developments which covers from the image receptor until mechanical structure. Current equipment are compact and provides a varied field of view (FOV) that allows image acquisition from a single dental unit to the entire face. Currently CBCT offers two options for acquiring full dental arcade images: (1) use of a diameter of FOV encompassing full arcade, single FOV protocol;

(2) using a combination of several images from sectorized dental units, stitched FOV protocol.

All technological options adopted for diagnosis in humans must comply with the diagnostic purpose and their image quality should provide the maximum possible information about the area being examined. At the same time, radiological protection of patients means one should always obtain exposures that meet the ALARA principle by being 'as low as reasonably achievable' (Endo et al., 2013; Batista et al., 2012, 2013).

In reality, it is difficult to conduct comparative studies of effective doses as the technologies of the available equipment vary. These difficulties mainly comprise differences in the exposure parameters, filtration, volumes and geometries used. In the literature, the results are very different and are probably associated with these differences (Roberts et al., 2009; Rottke et al., 2013; Qu et al., 2010).

<sup>☆</sup>In this paper, this technique is called single FOV protocol.

\* Corresponding author. Fax: +55 71 2102 9412.

E-mail address: [mrs2206@gmail.com](mailto:mrs2206@gmail.com) (M.R. Soares).

Recent studies have calculated the absorbed dose in organs/tissues and the effective dose by Monte Carlo computer simulation (Morant et al., 2013). Others use thermoluminescent dosimeters (TLD) (Pauwels et al., 2012) or semiconductors (MOSFET) (Koivisto et al., 2012) in anthropomorphic phantoms.

In this context, this study aimed at assessing single FOV protocols and stitched FOVs that have a similar clinical purpose by using estimates of effective dose.

## 2. Materials and methods

### 2.1. Anthropomorphic phantom

In this study a female Alderson anthropomorphic phantom manufactured by Radiology Support Devices was used. The phantom represents a typical adult woman 1.6 m in height and weighing 55 kg (Goren et al., 2013). It consists of a human skeleton filled with material of atomic mass equivalent to human soft tissue. Ten slices with a thickness of 2.5 cm, as shown in Fig. 1, were used. The slices had various cylindrical holes filled with rods. Each dowel had an appropriate space, 3 mm × 3 mm × 1 mm, for placing of dosimeters.

### 2.2. Protocols used

To acquire an image of a full dental arch, it is necessary to use a FOV large enough to cover the entire length of the arch diameter. Using the equipment that has the option of imaging with large diameters, the acquisition is performed in a single exposure. The present paper, this technique is called single FOV protocol, presented in Fig. 2(a) and (b). However, with the purpose of reducing the final cost of the product, some models of CBCT available on the market do not have image receptor of sufficient size for the acquisition of all the dental arcade in a single exposure. A software-based alternative is the acquisition of multiple images which are electronically joined later. This technique is named by manufacturers “stitched”, and it is presented in Fig. 2(c) and (d).

### 2.3. Equipment used and protocol assessment

Four pieces of CBCT equipment and five different protocols were used. The techniques used to acquire images of the two dental arches, lower jaw and upper jaw, or just the upper arch, were in accordance with the protocols. The equipment included in



Fig. 1. Head and neck of anthropomorphic phantom representing an typical adult woman.

this study and its characteristics are shown in Table 1. In all exposures a typical patient was treated with predefined protocols by equipment normally used for routine imaging. An i-CAT Classical and Gendex GXCB 500 equipmet performed the single FOV (protocols [a], [b] and [e] respectively). A CS 9000 3D™ CBCT equipment for the 5 cm × 3.7 cm (diameter × height) FOV, the old Kodak 9000™, and Planmeca ProMax™ 3D for the FOV of 5 cm × 8 cm (diameter × height) performed stitched FOVs (protocols [c] and [d] respectively).

In all exposures, the TLDs were in the same positions in the phantom. The position of the phantom in the CT scanners for each exposure was performed with the aid of laser beams locators and with professional help. The radiation emitted in the preview was also taken into account to obtain the estimated effective dose.

### 2.4. Thermoluminescent dosimeters

Twenty-six thermoluminescent dosimeters were used (TLD-100 consisting of LiF: Mg, Ti). TLDs were calibrated using known exposure parameters, ranging from 1 to 15 mGy in diagnostic radiology qualities, with computed tomography protocols (RQT8, RQT9 and RQT10). Industrial X-ray equipment was used for calibration such as, a Pantak/Seifert 160HS ISOVOLT. All readings (calibration and measurements) were performed on a Harshaw TLD reader, model QS 3500, with the aid of WinREMS software coupled to a data acquisition system.

The process of the initiation of the calibration until the determination of the dose in organs and tissues, for the selected dosimeters consisted of the following steps: (i) obtain the sensitivity factor, ~1.1, correcting the homogeneity of the set of dosimeters; (ii) irradiation of the dosimeters with X-rays in air, at a distance of 1 m from the source of radiation, in the quality RQT 9, with values in the range of 1–15 mGy; (iii) conversion of the readings of the dosimeters in absorbed dose in organs/tissues of the phantom was calculated through dose response calibration curve ( $Dose = 0.0634 \times TL_{reading}$ ), in which, is included the ratio  $(\mu/\rho)_{air}$  the mass–energy absorption coefficients for air and  $(\mu/\rho)_T$  for tissue, 1.1133 for soft tissue, (Gonzaga et al., 2014); (iv) assessment of the, uncertainties estimated through the standard deviation, with a lower value than 10%.

### 2.5. Location of TLDs and irradiation simulator

The selection of tissues and organs was based on the methodology presented by Ludlow et al. (2006) and Roberts et al. (2009) incorporating the new definitions outlined in ICRP (2007). In total, eight organs and tissues were selected for evaluation.

For the location of tissues so that organs the support of an oral radiologist was used. For each protocol three exposures were carried out and the response of the dosimeter was divided by three. A position and a slice number of each dosimeter are summarized in Table 2.

### 2.6. Calculation of the effective dose

The effective dose values were obtained using Eq. (1):

$$E = \sum_T H_T w_T \quad (1)$$

where  $H_T$  is equivalent dose, Eq. (2)

$$H_T = w_R \sum_i f_i D_{T,i} \quad (2)$$

where  $w_R$  is the radiation weighting factor ( $w_R = 1$  Sv/Gy for X-rays),  $f_i$  is the mass fraction of the tissue  $T$  that has been irradiated on the location/slice  $i$ ,  $D_{T,i}$  the absorbed dose averaged over tissue  $T$ , on the slice  $i$ , once the dose value associated to some

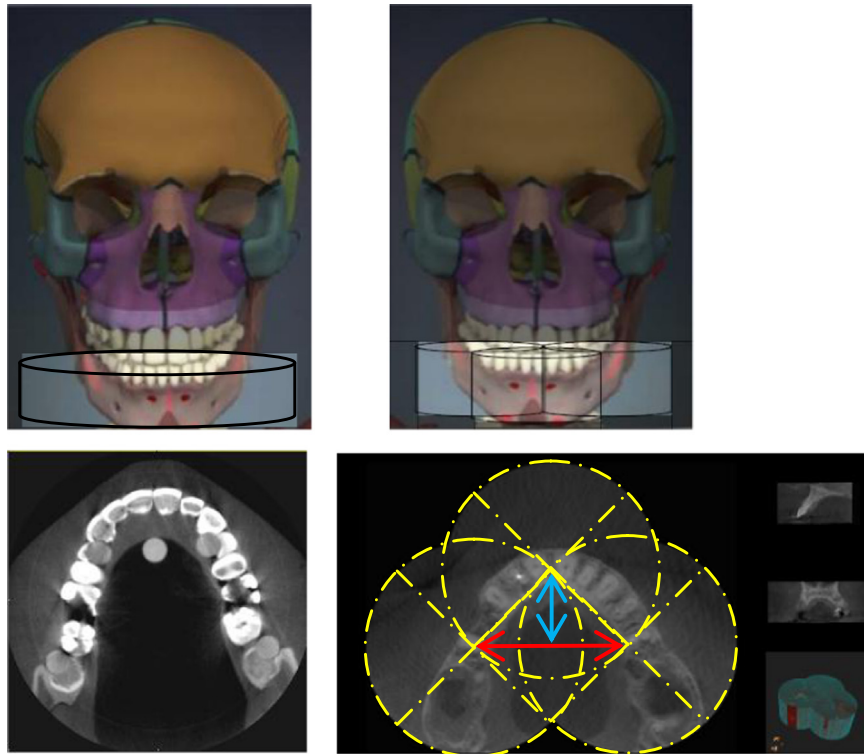


**Fig. 2.** Protocols for image acquisition of the entire arch. (a) Representing the single FOV protocol; (b) resulting image of a single FOV protocol; (c) representation of multiple FOVs; (d) image resulting from a of multiple FOVs protocol.

**Table 1**  
Technical characteristics of the equipment and parameters used for exposure of the phantom.

Equipment	Protocol	FOV <sup>1</sup> (cm)	Angle (deg)	Kilovoltage (kV)	Current (mA)
Gendex GXCB 500 <sup>TM</sup>	[a]	∅14 × 8.5	360	120	5
Gendex GXCB 500 <sup>TM</sup>	[b]	∅ 8.5 × 8.5	360	120	5
CS 9000 <sup>TM</sup>	[c]	∅ 5 × 3.7	360	70	8
Promax <sup>TM</sup> 3D	[d]	∅ 5 × 8	210	84	12
i-CAT Classi- cal <sup>TM</sup>	[e]	∅ 16 × 8	360	120	3–7

1-Values in cm. First value corresponds to the diameter of the FOV second value and the height of the FOV.

organs/tissues can be obtained from results dosimeters placed in different slices i.(Koivisto et al., 2012; Roberts et al., 2009; Rottke et al., 2013). Table 3 shows that these fractions were estimated as: 10% of the oesophagus; 5% of the total body skin on the surface area of the head/neck, lymphatic nodes and muscle; 16.5% bone marrow and bone surface and 100% for other organs/tissues (Koivisto et al., 2012; Ludlow et al., 2003).

The weighting factor,  $w_T$  used for organs and tissues where taken from ICRP 103 (ICRP, 2007), described in Table 3.

### 3. Results

The results obtained in this study indicated that effective dose value is in the range of 43.1  $\mu$ Sv and 111.5  $\mu$ Sv for CBCT equipment using single FOV protocols ([a], [b] and [e]) and in the range of 44.5 and 236.2  $\mu$ Sv for CBCT equipment using protocols with stitched FOVs ([c] and [d]). The results of each protocol are presented in Table 4.

**Table 2**  
Location of the TLDs in the slices of the phantom.

N° TLD	Location
1	Surface of the left side (5) *
2	Posterior neck (5) *
3	Left thyroid (8) *
4	Right lens (3) *
5	Left lens (3) *
6	Posterior calvarium (2)
7	Calvarium right (2)
8	Calvarium left (2)
9	Anterior calvarium (2)
10	Middle point of the brain (2)
11	Pituitary gland (3)
12	Right orbit (3)
13	Left orbit (3)
14	Centre of the spinal column (5)
15	Right parotid (5)
16	Right branch (5)
17	Left parotid (5)
18	Branch left (5)
19	Centre of the sublingual gland (6)
20	Right submandibular (6)
21	Left submandibular (6)
22	Right mandible (6)
23	Left mandible (6)
24	Oesophagus (9)
25	Right thyroid (9)
26	Left thyroid (9)

\* Surface of phantom

Protocol [c] allows only the realization of the image of the lower or upper jaw at any one time. Other protocols ([a], [b], [d] and [e]) allow the visualization of the upper and lower jaw simultaneously. The highest estimated effective dose was presented by protocol [d] and the smallest by protocol [a]. Fig. 2(a) clearly shows areas of interception among the three fields of radiation of the stitched FOV protocol. Fig. 2(c) shows the arrangement of the

**Table 3**

ICRP 103 (ICRP, 2007) Weighting Factor tissue,  $w_T$ , fraction irradiated,  $f_i$ , and dosimeters used to calculate the effective dose.

Organ/Tissue	Weighting factor ( $w_T$ )	$f_i$	Dosimeter
Bone marrow	0.12	0.165	
Calvaria	0.118	6, 7, 8, 9, 12, 13	
Centre of the spinal column		0.034	14
Mandible		0.012	16, 18, 22, 23
Eosophagus	0.04	0.1	24
Thyroid	0.04	1	3, 25, 26
Skin	0.01	0.05	1, 2, 3, 4
Bone surface <sup>a</sup>	0.01	0.165	
Brain	0.01	1	9, 10
Salivary glands	0.01	1	
Parotid			15, 17
Submandibular			20, 21
Sublingual gland			19
Remaining tissues	0.12		
Lymphatic nodes		0.05	15, 17, 19, 20, 21
Extrathoracic airway		1	12,13, 15, 17, 24, 25, 26
Muscle		0.05	15, 17, 19, 20, 21
Oral Mucosa		1	16, 15, 17, 18, 19, 20, 21, 22, 23

<sup>a</sup> Bone surface dose = Bone marrow dose  $\times$  3.23.

**Table 4**

Estimation of effective dose using anthropomorphic female phantom.

Exposure technique	Protocol	Effective dose, ( $\mu$ Sv)
Single FOV	[a]	43.1
Single FOV	[b]	52.0
Stitched FOVs	[c]	44.5
Stitched FOVs	[d]	236.2
Single FOV	[e]	111.1

single FOV protocol in the cross-sectional image.

#### 4. Discussion

There is a variety of CBCT equipment available on the market (Rottke et al., 2013), and each piece of equipment has particularities in terms of exposure parameters (kilovoltage, milliamperes, time, and filtration). It is necessary to evaluate the effective dose for all protocols associated with radiological procedures (Pauwels et al., 2012).

Usually, to estimate the effective dose, a male anthropomorphic phantom is used (Ludlow et al., 2006; Pauwels et al., 2012; Qu et al., 2012). This study, however, used a female anthropomorphic phantom. Comparison of these results with those of other studies should take into account that the male phantom is different from the female phantom in the dimensions of the face. Nevertheless, a recent study conducted with Monte Carlo simulation (Morant et al., 2013) using male and female mathematical phantoms found a higher equivalent doses for all organs and tissues for the female phantom results, except for the brain. The authors of this study (Morant et al., 2013) inferred the importance of considering age and sex in assessment of radiological risk.

When conducted a study on male, female and child physical phantoms Prins and colleagues found that the value of equivalent dose in the eye and brain showed no significant differences (Prins et al., 2011).

The present evaluation provides experimental data acquired in four different cone beam CT scanners that can be compared with the results from computer simulation and used to present data for

the average effective dose for both sexes as per ICRP 103 (ICRP, 2007).

In this study, the objective was to compare effective dose values for two different imaging techniques for complete arch. For the stitching technique, dose value was higher than for the single FOV technique the effective dose for protocol [d] is five times higher than the effective dose for protocol [a] and twice as high as that of protocol [e].

The results presented by protocol [d] are in accordance with a recent study by Qu et al. (2010). The effective dose measured, by Qu et al. (2010) in the male phantom was 216  $\mu$ Sv. In this study using the female simulator, an effective dose of 236  $\mu$ Sv was calculated. This difference may be related to the dimensions of the phantom or calibration factors of the equipment.

For protocol [a], the value of an effective dose of 43.1  $\mu$ Sv was obtained. This value is 15% less than for protocol [b] and 58% lower than for protocol [e]. Protocols [a], [b] and [e] use the same technique of image acquisition and it is possible to acquire the image of both arches at the same time. Thus protocol [a] has a significant advantage over protocols [b] and [e]. Another factor to be taken into consideration is that in protocol [c] it is only possible to obtain the image of the lower or upper jaw at any one time. Analysis of the results of Table 4 shows that the dose value derived from protocol [c] is almost equal to that obtained for protocol [a]. In this case, protocol [c] does not offer any advantage because to acquire the image of both dental arches it is necessary to perform the same protocol twice ( $2 \times$  protocol [c]). Of course, the amount of irradiated tissue should also be taken into consideration. In this sense, protocol [c] is more specific. If, however, the goal is to obtain an image of both dental arches the present results indicate that the best option is to use single FOV protocols.

In Fig. 2(d), there is an evident overlap between the fields of radiation, which can cause overexposure in some organs/tissues.

#### 5. Conclusion

It can be concluded that, in terms of the value of effective dose, stitched protocols [c] and [d] do not have any advantage over other protocols. These facts suggest the necessity for knowledge of the exposure parameters and effective dose values associated with each image protocol to assist the radiologist in making a decision.

#### References

- Batista, W.O., Navarro, M.V.T., Maia, A.F., 2013. Development of a phantom and a methodology for evaluation of depth Kerma and Kerma index for dental cone beam computed tomography. *Radiat Prot Dosimetry* 157 (4), 543–551.
- Batista, W.O.G., Navarro, M.V.T., Maia, A.F., 2012. Effective doses in panoramic images from conventional and cbct equipment. *Radiat Prot Dosimetry* 151 (1), 67–75.
- Endo, A., Katoh, T., Vasudeva, S.B., Kobayash, I., Okano, T., 2013. A preliminary study to determine the diagnostic reference level using dose-area product for limited-area cone beam CT. *Dentomaxillofacial Radiology* 42 (4), 20120097.
- Gonzaga, N.B., Mourão, A.P., Magalhães, M.J., da Silva, T.A., 2014. Organ equivalent doses of patients undergoing chest computed tomography: measurements with TL dosimeters in an anthropomorphic phantom. *Appl Radiat Isot* 83, 242–244.
- Goren, A.D., et al., 2013. Effect of leaded glasses and thyroid shielding on cone beam CT radiation dose in an adult female phantom. *Dentomaxillofacial Radiol.* 42, 20120260.
- ICRP, 2007. Recommendations of the International Commission on Radiological Protection. ICRP Publication 103, p. 332 (International Commission on Radiological Protection).
- Koivisto, J., Kiljunen, T., Tapiovaara, M., Wolff, J., Kortesiemi, M., 2012. Assessment of radiation exposure in dental cone-beam computerized tomography with the use of metal-oxide semiconductor field-effect transistor (MOSFET) dosimeters and Monte Carlo simulations. *Oral Surgery, Oral Medicine, Oral Pathology and Oral Radiology* 114 (3), 393–400.
- Ludlow, J.B., Davies-Ludlow, L.E., Brooks, S.L., 2003. Dosimetry of two extraoral direct digital imaging devices: NewTom cone beam CT and Orthophos Plus DS

- panoramic unit. *Dento maxillo facial radiology* 32 (4), 229–234.
- Ludlow, J.B., Brooks, S.L., Davies-Ludlow, L.E., Howerton, B., 2006. Dosimetry of 3 CBCT devices for oral and maxillofacial: CB Mercuray, NewTom 3G and i-CAT. *Dento maxillo facial radiology* 35, 219–226.
- Morant, J., Salvadó, M., Hernández-Girón, I., Casanovas, R., Ortega, R., Calzado, A., 2013. . Dosimetry of a cone beam CT device for oral and maxillofacial radiology using Monte Carlo techniques and ICRP adult reference computational phantoms. *Dentomaxillofacial Radiol* 42 (3), 92555893.
- Mozzo, P., Procacci, C., Tacconi, A., Tinazzi, Mar, 1998. A new volumetric CT machine for dental imaging based on the cone-beam technique: preliminary results. *Eur. Radiol.* 8 (9), 1558–1564.
- Pauwels, R., et al., 2012. Effective dose range for dental cone beam computed tomography scanners. *Eur. J. Radiol.* 81 (2), 267–271.
- Prins, R., et al., 2011. Significant reduction in dental cone beam computed tomography (CBCT) eye dose through the use of leaded glasses. *Oral Surgery, Oral Medicine, Oral Pathology, Oral Radiology and Endodontics* 112 (4), 502–507.
- Qu, X.M., Li, G., Sanderink, G.C.H., Zhang, Z.Y., Ma, X.C., 2012. Dose reduction of cone beam CT scanning for the entire oral and maxillofacial regions with thyroid collars. *Dentomaxillofacial Radiology* 41 (5), 373–378.
- Qu, X.M., Li, G., Ludlow, J.B., Zhang, Z.Y., Ma, X.C., 2010. Effective radiation dose of ProMax 3D cone-beam computerized tomography scanner with different dental protocols. *Oral Surgery, Oral Medicine, Oral Pathology, Oral Radiology and Endodontics* 110 (6), 770–776.
- Roberts, J.A., Drage, N.A., Davies, J., Thomas, D.W., 2009. Effective dose from cone beam CT examinations in dentistry. *The British Journal of Radiology* 82 (973), 35–40.
- Rottke, D., Patzelt, S., Poxleitner, P., Schulze, D., 2013. Effective dose span of ten different cone beam CT devices. *Dentomaxillofacial Radiology* 42, 20120417.